Oncogene
https://doi.org/10.1038/s41388-020-1172-0

ARTICLE

Preclinical validation of Alpha-Enolase (ENO1) as a novel immunometabolic target in multiple myeloma

Arghya Ray[1] · Yan Song[1] · Ting Du[1] · Dharminder Chauhan[1] · Kenneth C. Anderson[1]

Received: 4 November 2019 / Revised: 7 January 2020 / Accepted: 20 January 2020

Abstract

Bone marrow plasmacytoid dendritic cells (pDCs) in patients with multiple myeloma (MM) promote tumor growth, survival, drug resistance, and immune suppression. Understanding the molecular signaling crosstalk among the tumor cells, pDCs and immune cells will identify novel therapeutic approaches to enhance anti-MM immunity. Using oligonucleotide arrays, we found that pDC-MM interactions induce metabolic enzyme Alpha-Enolase (ENO1) in both pDCs and MM cells. Analysis of MM patient gene expression profiling database showed that *ENO1* expression inversely correlates with overall survival. Protein expression analysis showed that ENO1 is expressed in pDC and MM cells; and importantly, that pDC-MM coculture further increases ENO1 expression in both MM cells and pDCs. Using our coculture models of patient autologous pDC-T-NK-MM cells, we examined whether targeting ENO1 can enhance anti-MM immunity. Biochemical inhibition of ENO1 with ENO1 inhibitor (ENO1i) activates pDCs, as well as increases pDC-induced MM-specific $CD8^+$ CTL and NK cell activity against autologous tumor cells. Combination of ENO1i and anti-PD-L1 Ab or HDAC6i ACY-241 enhances autologous MM-specific $CD8^+$ CTL activity. Our preclinical data therefore provide the basis for novel immune-based therapeutic approaches targeting ENO1, alone or in combination with anti-PD-L1 Ab or ACY241, to restore anti-MM immunity, enhance MM cytotoxicity, and improve patient outcome.

Introduction

Recent advent of novel therapies has markedly prolonged the survival in patients with Multiple Myeloma (MM); however, therapies with novel mechanisms of action are needed due to the development of drug-resistance and relapse of disease [1–3]. A major factor contributing to either de novo or acquired resistance to therapies is the host-MM bone marrow (BM) microenvironment. One such mechanism whereby the BM microenvironment promotes tumor progression is by altering tumor cell metabolism [4, 5]. Indeed, studies in other cancers have reported alterations in tumor cell metabolism in the tumor microenvironment [5–9]. Specifically, tumor cells under physiological stress in the BM niche preferentially utilize aerobic glycolytic pathway versus mitochondrial respiration (oxidative phosphorylation) for energy production to meet the increased requirements for lipid and protein synthesis: for adaptation to variable nutrients and low oxygen levels; as well as for proliferation and survival [5, 6, 8–10]. This phenomenon is a hallmark of cancer and is described as the ''Warburg effect'' [4, 5].

Earlier studies showed that hypoxia in the tumor BM microenvironment contributes to reprogramming of tumor cell metabolic pathways [5–9, 11]. In MM, hypoxia-triggered hypoxia inducible factor-1 (HIF-1α) activates glycolytic pathway; HIF-1α and its target LDHA in turn are associated with drug-resistance in MM [11]. In MM, a recent study showed a role of HIF-1α and KDM3A (an H3K9 demethylating enzyme) and its downstream target MALAT1 (a long noncoding RNA) in regulating glycolytic metabolic pathway and oncogenesis [12]. Additionally, studies in solid tumors showed a correlation of elevated HIF-1α levels with metastasis and shorter patient survival [13, 14]. Together, these findings suggest the potential of

Joint senior authors: Dharminder Chauhan, Kenneth C. Anderson

✉ Dharminder Chauhan
Dharminder_Chauhan@dfci.harvard.edu

✉ Kenneth C. Anderson
Kenneth_Anderson@dfci.harvard.edu

[1] Department of Medical Oncology, The LeBow Institute for Myeloma Therapeutics and Jerome Lipper Myeloma Center, Dana Farber Cancer Institute, Harvard Medical School, Boston, MA, USA

Published online: 05 February 2020

targeting tumor cell metabolism in the BM milieu to overcome drug-resistance.

Interactions among various BM accessory cells, immune cells, and tumor cells confer growth, survival, drug resistance, and immune suppression in MM cells [3]. Our studies provide one such example of interactive mechanism(s) between MM cells and BM accessory cells in mediating MM progression. Specifically, we found that plasmacytoid dendritic cells (pDCs) are immunologically dysfunctional and play a pathophysiological role in MM [15]. Using both in vitro and in vivo models of human MM in the BM milieu, we identified increased numbers and more frequent localization of pDCs in MM patient BM. Importantly, pDC-T-NK-MM cells interactions stimulate tumor proliferation, chemoresistance, and immune suppression [15–19]. Our preclinical studies have also identified several molecular mechanism(s) including immune checkpoints mediating pDC-MM interactions; conversely, we have validated checkpoint inhibition to restore pDC immune function and inhibit MM cell growth [15–19]. In concert with our studies, a recent study using Vk*MYC myeloma mouse model showed a role of pDCs in MM progression [20]. To date, however, a role of pDC-MM interactions in modulating metabolic pathways in MM cells has not been delineated.

In this study, we utilized our co-culture models of pDCs and MM cells to examine the genetic changes in MM cells. We found that pDCs interactions with MM cells significantly upregulate metabolic pathway-related gene alpha-enolase (ENO1) in both MM cells and pDCs. ENO1 is a glycolytic enzyme mediating conversion of 2-phospho-D-glycerate to phosphoenolpyruvate in the final step of the glycolytic pathway [21–23]. To determine the functional significance of ENO1, we utilized our pDC-T-NK-MM cells co-culture models to show that targeting ENO1 stimulates MM cytotoxic T lymphocyte (CTL)- and NK-cell activity. Moreover, the combination of ENO1 inhibitor with either anti-PD-L1 Ab or HDAC6i ACY241 restores anti-MM immune responses and enhances MM cytotoxicity. Our data therefore provide evidence for a role of metabolic enzyme ENO1 in immune modulation, and provide the preclinical rationale for therapeutic targeting of ENO1-mediated glycolytic pathway to enhance tumor cytotoxicity and improve patient outcome in MM.

Results and discussion

pDCs trigger transcription of glycolysis pathway enzyme ENO1 in MM cells

Gene expression profiling of MM.1S cells cocultured with MM patient pDCs showed that pDCs trigger alterations in transcription of metabolic pathway-related genes in MM cells (Fig. 1a). For example, pDCs upregulate alpha-enolase (*ENO1*), a key molecule in the aerobic glycolytic pathway, in MM cells (Fig. 1a, b; 1.8-fold increase versus MM alone; $n = 3$; CI > 95%). Reverse transcription–qPCR (RT–qPCR) analysis confirmed higher *ENO1* levels in MM cells cocultured with pDCs versus MM alone. (Fig. 1c). While we found alterations in other metabolism-associated genes (e.g. PKM2, CS, IDH1, ACO2, FH, MDH2, or HK1)), we focused on examining the functional significance of ENO1 in the present study since: (1) a significant induction of ENO1 was noted during pDC-MM interactions versus other molecules; (2) ENO1 is essential for maintaining tumor cell metabolism and represents a potential therapeutic target in cancer [21–24]; (3) ENO1 promotes tumor cell proliferation and cell adhesion-mediated drug-resistance (CAM-DR) [25] characteristic of MM; and (4) ENO1 functions as an immunoregulatory molecule both in T-regulatory cell differentiation and dendritic cell function [23, 24].

Clinical relevance of *ENO1* expression in MM

We next examined the *ENO1* gene expression in samples from normal healthy individuals, individuals with monoclonal gammopathy of undetermined significance (MGUS), and patients with active MM. *ENO1* levels are significantly higher in individuals with MGUS ($p < 0.05$) or in MM patients ($p < 0.01$) versus normal healthy donor plasma cells (Fig. 1d). Using publicly available GEP database (Study 1; Series GSE6477), we further examined *ENO1* expression in patients receiving total therapy 2 (TT2) [26]. As shown in Fig. 1e, patients with high *ENO1* expression showed poor overall survival versus low-*ENO1*-expressing patients ($p = 0.012$). These findings are consistent with prior reports showing correlation between high ENO1 expression and shorter survival in cancer patients [21, 27]. Importantly, earlier GEP studies in MM showed a correlation of *ENO1* expression with poor outcome [28–31]. These data suggest that ENO1 plays an important role in MM pathogenesis.

To determine whether pDC-induced *ENO1* gene levels in MM cells correlate with alterations in ENO1 protein expression, we cocultured freshly isolated MM patient pDCs with autologous tumor cells, and analyzed ENO1 expression using flow cytometry. Both MM cells and pDCs express ENO1; and importantly, pDC-MM cell coculture further increases ENO1 expression on MM cells ($p = 0.0115$) (Fig. 2a), and triggers a significant increase in $ENO1^+$ MM cells (three fold; $p < 0.001$) (Fig. 2b). Importantly, analysis of pDCs after coculture with MM cells also shows a significant increase in ENO1 expression (MFI: three-fold increase in pDCs cultured with MM versus pDCs

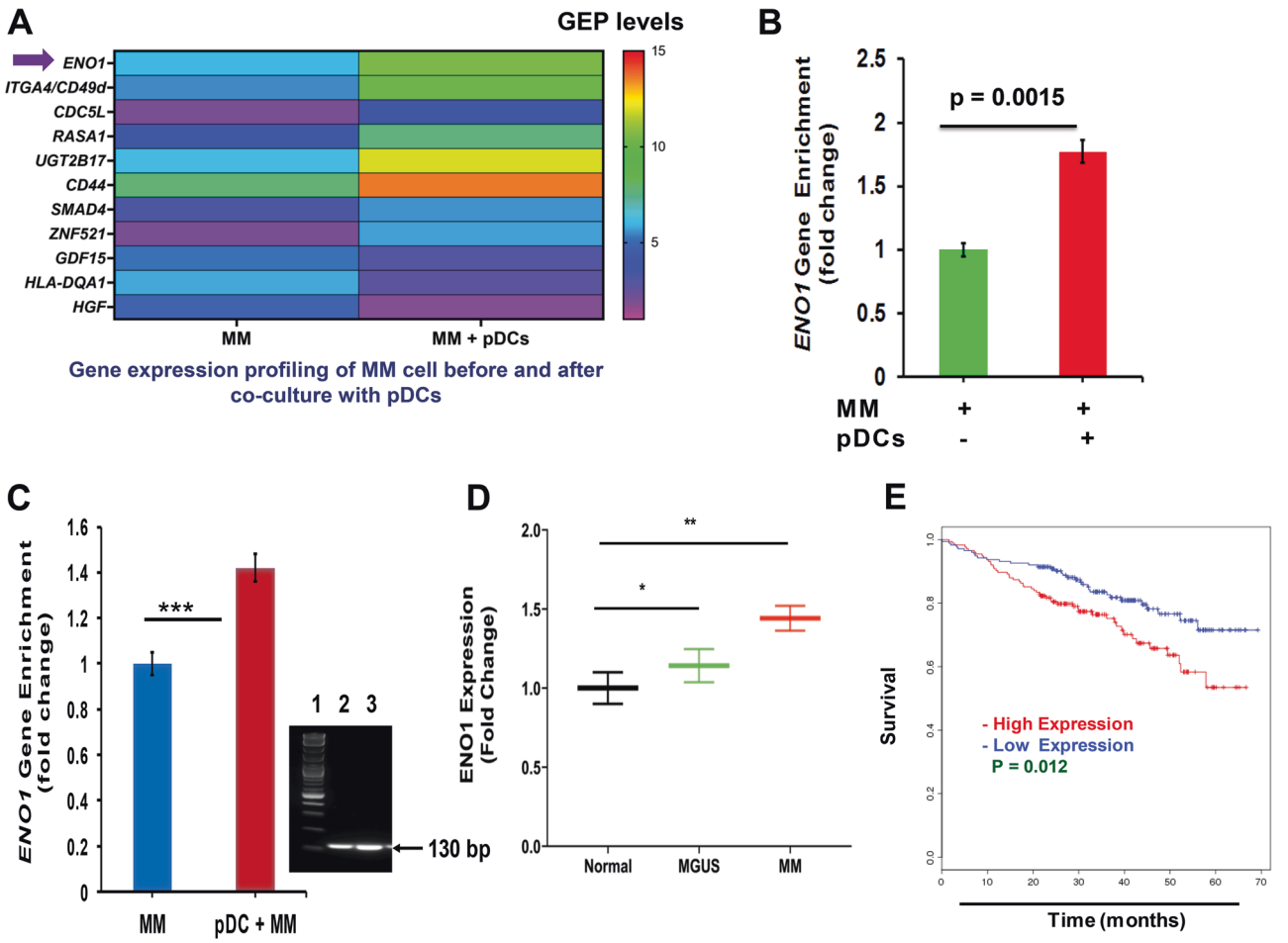

Fig. 1 Gene expression profiling of MM cells in the presence or absence of pDCs. a Oligonucleotide array analysis: MM cells were cocultured with pDCs for 48 h, separated using anti-CD138 antibody and flow sorting, and harvested. Poly RNA was subjected to microarray analysis using HG-U133 plus 2.0 plus Affymetrix chip. Data processing: the CEL files were obtained using Affymetrix Microarrays Suite 5.0 software. GeneChip 5.0 (Affymetrix, Santa Clara, CA) was utilized to scan, quantify, and analyze the scanned image. GeneChip software automatically calculated intensity values for each probe cell, and marked a presence or absence call for each mRNA. Algorithms in the software used probe cell intensities to calculate an average intensity for each set of probe pairs representing a gene, which correlates with the amount of mRNA. Gene expression patterns for MM cells cultured in the presence vs absence of pDCs were compared, and a heat map was generated (>1.5-fold change in transcript is considered significant, CI > 95%). The expression profile of *ENO1* transcript is shown. **b** Quantification of ENO1 expression: normalized *ENO1* gene enrichment in pDC-MM cell co-culture versus MM cells alone is presented [1.772-fold upregulation; $n = 3$; CI > 95%]. **c** Validation and Quantification of ENO1 gene expression by RT-qPCR: MM cells were cocultured with pDCs for 48 h; separated using anti-CD138 antibody and flow sorting, and harvested. Poly RNA was subjected to RT-qPCR using Luna Universal 1-step RT-qPCR kit (New England BioLabs, MA, USA) following manufacturer protocol using an Applied Bioscience 7500 Fast Real-Time PCR System (Thermo Scientific Inc). ENO1 gene expression was quantified from the raw data using ΔΔCT and utilizing GAPDH as the housekeeping reference gene control. The bar graph denotes ENO1 gene expression in MM cells cultured in the presence vs absence of pDCs (mean ± SD; $p < 0.05$). Inset: Analysis of qPCR amplicons (130 bp) on a 2.5% agarose gel stained with GelRed Nucleic Acid Gel Stain (Biotium Inc, USA). Lane-1: 1 kb DNA ladder; Lanes-2 and −3: ENO1 expression in MM cultured in the absence and presence of pDCs, respectively. **d** Expression data from different stages of plasma cell neoplasm collected using Affymetrix Human Genome U133A [HG-U133A] Array platform based on NORMAL ($N = 4$), MGUS ($N = 11$), and multiple myeloma (MM: $N = 73$) samples. The data is presented as fold change (FC) in each group versus normal. **e** Survival analysis of TT2 MM patient cohorts based on high and low expression of *ENO1* gene. The gene expression analysis is based on TT2 patients survival data collected using [HG-U133_Plus_2] Affymetrix Human Genome U133 Plus 2.0 Array platform. The survival difference between high vs low expression groups is significant for the duration of the study ($p = 0.012$). [Note D-E: The analysis of data was based on the information available on the following website: http://www.canevolve.org/AnalysisResults/AnalysisResults.html].

alone; $p = 0.008$) (Fig. 2c, scatter plot and bar graph). Coculture of pDCs from normal healthy donors also enhance ENO1 expression in MM cells, but to a much lesser extent than MM-patient pDCs (data not shown). Similar elevated levels of ENO1 have been observed in immunosuppressive myeloid-derived suppressor cells [32]. These data suggest that pDC-MM interactions may modulate glycolytic metabolism via ENO1 enzyme.

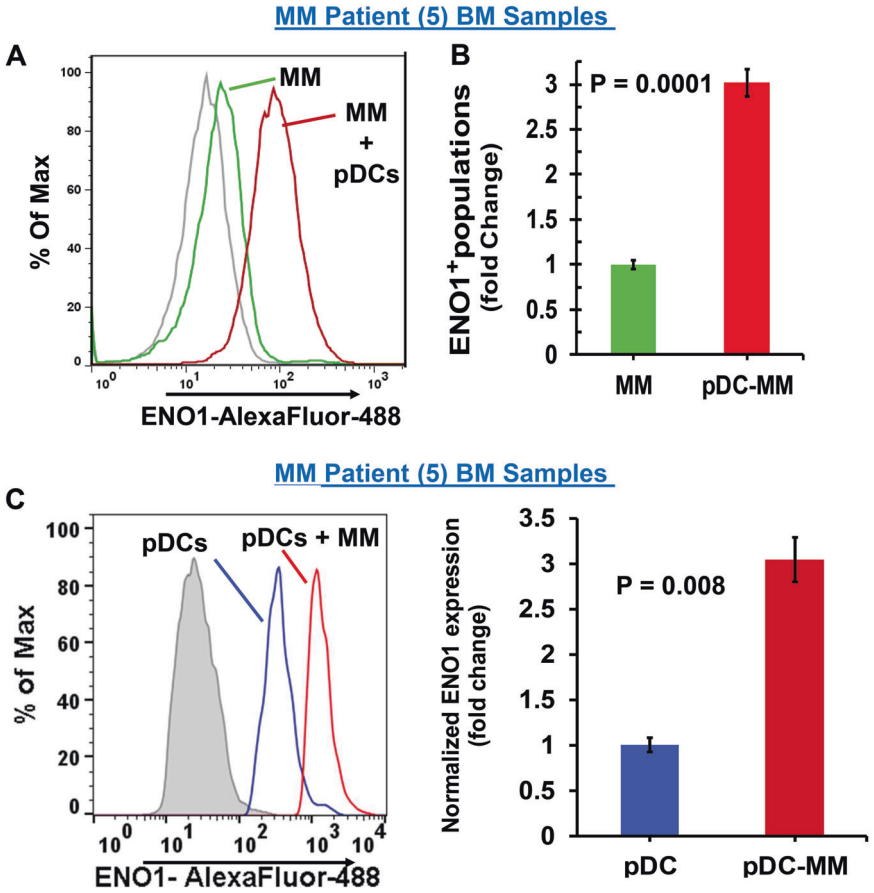

Fig. 2 Modulation of ENO1 expression during pDC-MM cell interactions. a pDCs were cocultured with autologous patient MM cells for 24 h, followed by multicolor flow analyses to assess the pDC-induced change in ENO1 expression on MM cells. $CD138^+$ MM cells were examined using flow cytometry, and Median Fluorescence Intensity (MFI) of ENO1 expression was determined using anti-ENO1 Ab conjugated to AlexaFluor-488, both in the presence or absence of pDCs. Representative histograms show ENO1 expression in MM cells cultured in the presence (red) and absence (green) of pDCs. [Black histogram: Isotype control Ab]. Data was quantified from the histogram analyses ($p = 0.0115$; $N = 5$ MM patient BM samples). **b** pDCs were cocultured with autologous patient MM cells for 24 h, followed by multicolor flow analysis to determine the pDC-induced change in the $ENO1^+$ MM cell population [mean ± SD; $p < 0.05$; $N = 5$ MM patient BM samples]. **c** MM BM-pDCs were subjected to multicolor flow analyses to determine the surface ENO1 expression on pDCs. pDCs ($CD304/CD123/CD303^+$) were gated and Median Fluorescence Intensity (MFI) was determined for surface ENO1 expression on pDCs using anti-ENO1-AlexaFluor-488 Ab. Representative histograms show ENO1 expression on MM-BM-pDCs (blue line) and BM-pDCs cocultured with MM cells (red line) [Shaded black histogram: Isotype control Ab]. ($N = 5$ MM patient BM samples).

ENO1 blockade triggers pDC activation and increases T cell proliferation

Our earlier studies showed that MM patient pDCs stimulate significantly less T cell proliferation than normal pDCs [15–17]. Our present finding that pDC-MM interactions upregulate ENO1 in pDCs, coupled with prior reports showing an immunoregulatory role of ENO1 in dendritic cell function [23, 24], suggested that ENO1 inhibition may improve MM patient pDCs immune function. Treatment of pDCs from MM patients with non-toxic (0.1 μM) concentrations of ENO1 inhibitor (ENO1i) activates pDCs, as evidenced by an increase in pDCs maturation/activation markers (CD80/CD83/CD40) (Fig. 3a–c). We next examined whether ENO1 inhibition in pDCs affects the biologic sequelae of pDC-T cell interactions. Treatment of MM-patient pDCs with ENO1i triggers proliferation of autologous T cells, as well as their activation by virtue of CD69 expression (Fig. 3d, $p = 0.016$; Fig. 3e, $p = 0.018$, respectively) These data show that blockade of ENO1 restores the ability of MM-patient pDCs to trigger autologous T cell proliferation and activation.

ENO1 inhibition induces pDC-triggered T and NK cell- mediated anti-MM activity

Our prior studies showed that pDCs activation/maturation can stimulate T and NK cell immune function in MM [15–19]. We next therefore examined whether blockade of ENO1 stimulates pDC-induced MM-specific CTL and NK cell activity ex vivo. These studies were performed using our

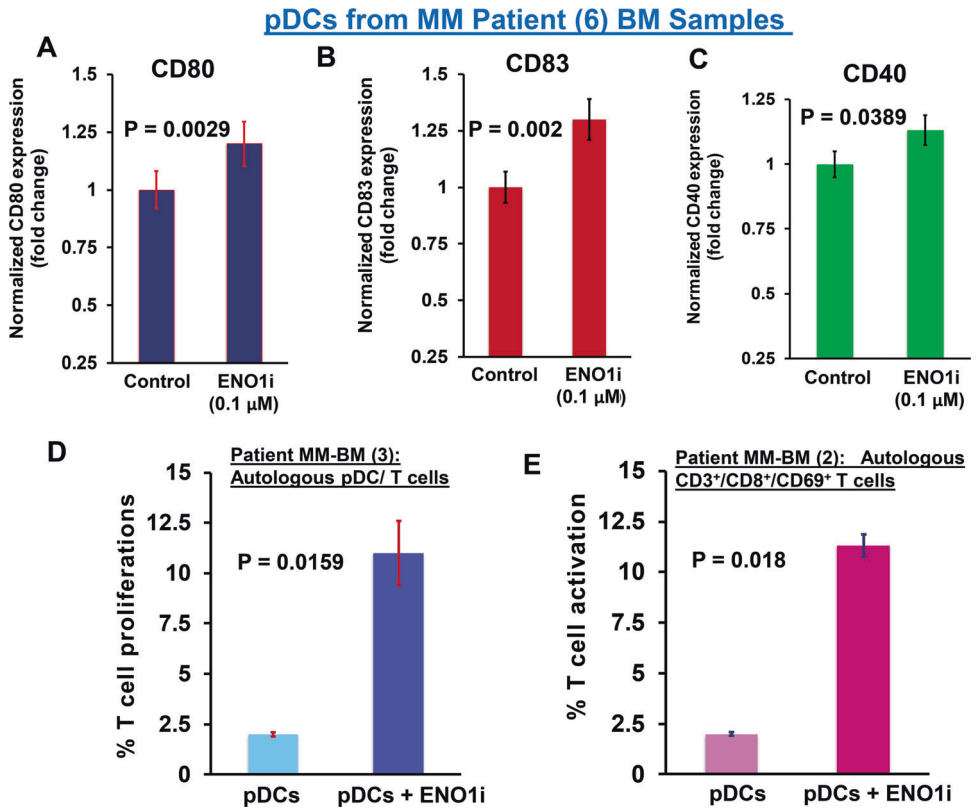

Fig. 3 ENO1 blockade activates pDCs and enhances pDC-triggered T cell proliferation. MM patient pDCs were treated with ENO1i (0.1 μM) for 24 h, followed by multicolor staining and flow analysis. Expression of pDC activation/maturation markers CD80 (**a**), CD83 (**b**), and CD40 (**c**) were assessed using flow cytometry. Fold change on treated versus untreated pDCs is presented [mean ± SD; $p < 0.05$; $N = 6$ MM patient samples]. **d** pDCs from MM patients were cocultured with autologous T cells at 1:10 (pDC:T) ratio in the presence or absence of ENO1i (0.1 μM) for 3 days, and viable $CD8^+$ T cells were quantified using CellTrace Violet-Cell proliferation Kit by FACS (mean ± SD; $P < 0.05$, $N = 3$ MM patient BM samples). **e** pDCs from MM patients were cocultured with autologous T cells at 1:10 (pDC:T) ratio in the presence or absence of ENO1i (0.1 μM) for 3 days. Viable $CD3^+/CD8^+$ T cells were analyzed for the expression of CD69 activation marker using anti-CD69 Ab conjugated to APC-Cy7, and quantified by FACS (mean ± SD; $P < 0.05$, $N = 2$ MM patient BM samples).

coculture models of freshly isolated patient pDCs, T cells or NK cells with autologous MM cells. We have previously utilized these models to validate immune checkpoint PD-1-PD-L1 signaling axis as a therapeutic target in MM; [15, 17] and excitingly, a recent clinical trial using pembrolizumab (targeting PD-1 receptor) showed complete remission in patients with high-risk smoldering MM [33]. MM patient BM CD8+ T or NK-cells were cocultured for 3 days with autologous pDCs ($n = 7$) at 1:10 (pDC:T/NK) ratio, in the presence or absence of ENO1i (0.1 μM). After washing to remove the ENO1i, cells were cultured for 24 h with autologous MM cells pre-stained with CellTracker Violet (E/T ratio: 10:1, T or NK/MM), followed by 7-AAD staining and quantification of MM cell lysis by FACS. ENO1i induces a significant MM-specific $CD8^+$ CTL activity, evidenced by decreased viable MM cells (Fig. 4a; scatter plot and bar graph; $p = 0.004$). Furthermore, ENO1i triggers increased $CD107a^+$ degranulated CD8+ CTLs (Fig. 4b, $p = 0.011$). Similarly, ENO1i induces significantly increased anti-MM NK cell activity (Fig. 5a, scatter plot and bar graph). Consistent with these data, ENO1i triggers increased $CD107a^+$ degranulated NK cells (Fig. 5b). Of note, 2 of the 7 patients in whom pDCs, T, or NK cells, and MM cells were studied had newly diagnosed untreated MM, and 5 patients had relapsed MM resistant to bortezomib, dexamethasone, and lenalidomide therapy.

We next utilized total BM-MNCs from MM patients ($n = 7$) to evaluate whether ENO1i triggers autologous anti-MM immune responses. ENO1i significantly reduces viable MM cells in total BM-MNCs (53% ± 4% decrease in viable $CD138^+$ cells; $p < 0.001$). These results show that blockade of metabolic pathway enzyme ENO1 in the MM BM microenvironment triggers autologous anti-MM activity, consistent with an immunosuppressive role of ENO1 during pDC-T-NK cells interactions. Taken together, our findings show that blockade of ENO1 activates pDCs and restores pDC-induced T- and NK cell- mediated cytolytic activity against MM cells.

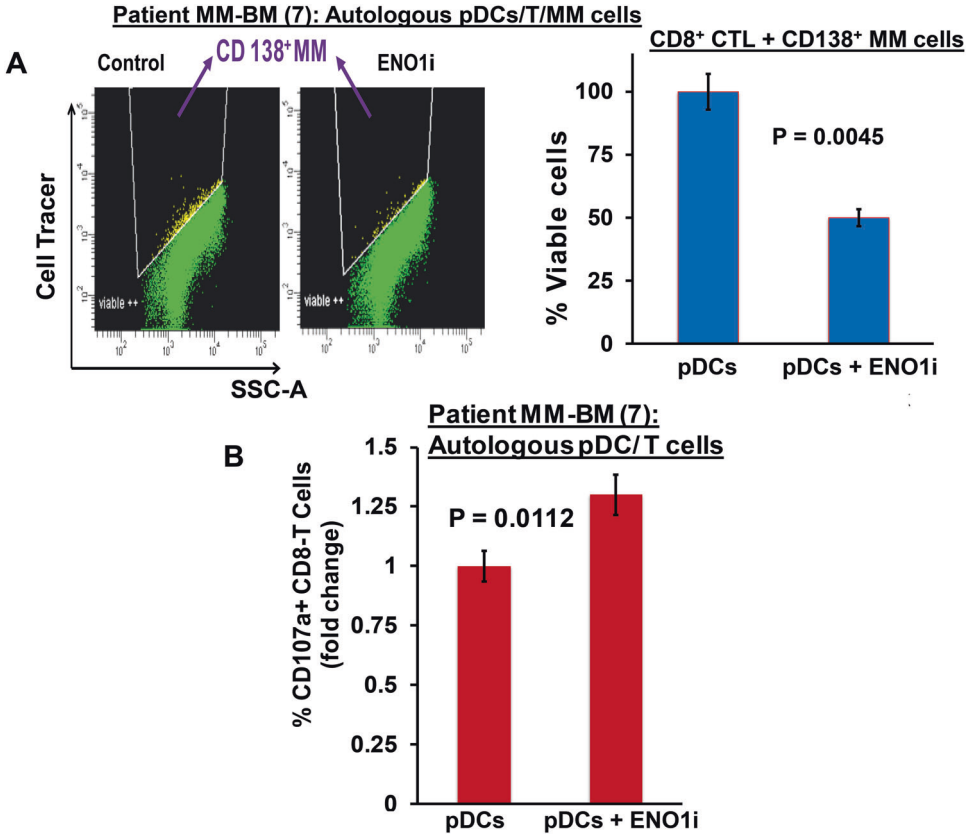

Fig. 4 ENO1 inhibition triggers pDC-induced MM-specific CD8+ CTLs. a MM patient BM $CD8^+$ T cells were cocultured with autologous pDCs ($N = 7$) at 1:10 (pDC: T) ratio in the presence or absence of ENO1i (0.1 μM) for 3 days. After washing to remove ENO1i, cells were cultured for 24 h with autologous MM cells prestained with CellTracker Violet (T/MM; 10:1 ratio), followed by 7-AAD staining and quantification of CTLs-mediated MM cell lysis by FACS. Left panel: representative FACS scatter plot showing the decrease in number of viable CellTracker-positive MM cells. Right panel: Bar graph shows quantification of $CD8^+$ CTLs-mediated MM cell lysis, reflected in CD138 + MM cell viability, using data obtained in left panel ($N = 7$ MM patient BM samples; mean ± SD; $p < 0.05$). **b** MM patient pDCs and autologous T cells (1:10 pDC/T ratio) were treated with DMSO control or ENO1i (0.1 μM), followed by degranulation assay to assess surface $CD107a^+$ T cells by multi-parameter flow cytometry. The plot shows percentage of surface $CD107a^+$ T cells, indicating degranulated CTLs ($N = 7$ MM patient BM samples; mean ± SD; $p < 0.05$).

Combination of ENO1i and anti-PD-L1 Ab or HDAC inhibitor ACY-241 enhances T cell-mediated MM-specific cytotoxic activity

Besides ENO1, pDC-MM interactions also upregulate immunosuppressive checkpoints including programmed cell death ligand-1 (PD-L1) [17–21]. Interestingly, a recent study in chronic lymphocytic leukemia showed that PD-1-PD-L1 axis contributes to dysfunction in metabolic pathways [34]. Whether PD-1-PD-L1 similarly affects ENO1, or vice versa, during pDC-MM interactions remains to be examined. Nonetheless, the fact that both ENO1 and PD-1-PD-L1 axis confer immune suppression suggests that combined blockade of ENO1 and PD-L1 may enhance induction of an anti-MM immune response. To assess this possibility, MM patient BM $CD8^+$ T cells ($n = 7$) were cocultured for 3 days with autologous pDCs (pDC:T; 1:10 ratio) in the presence of anti-PD-L1 Ab (5 μg/ml), ENO1i (0.1 μM), or ENO1i plus anti-PD-L1 Ab, and then evaluated in CTL assays against autologous MM cells (E:T ratio 10:1, T:MM), as in Fig. 5. The combination of ENO1i and anti-PD-L1 Ab triggers more robust autologous MM-specific CD8 + CTL activity than anti-PD-L1 Ab alone (Fig. 6a).

As for PD-1-PD-L1, histone deacetylases also modulate metabolic pathways [35]. A prior study showed that ENO1 is an HDAC-binding protein and may therefore be a target of HDACi [36]. We showed that the HDAC6 inhibitor ACY-241 can augment memory T cell and NK cell proliferation and cytotoxicity in MM [18, 37]. A clinical trial of ACY-241 and a peptide vaccine PVX-401 in smoldering MM (Clinical trial: NCT02886065) is ongoing. A Phase 1b study in non-small cell lung cancer utilizing ACY-241 and PD-1-targeting agent nivolumab has shown increased cytotoxic T and NK cell activity (Clinical trial: NCT02635061). These findings indicate that HDACi and ENO1i may enhance autologous anti-MM T and NK cell

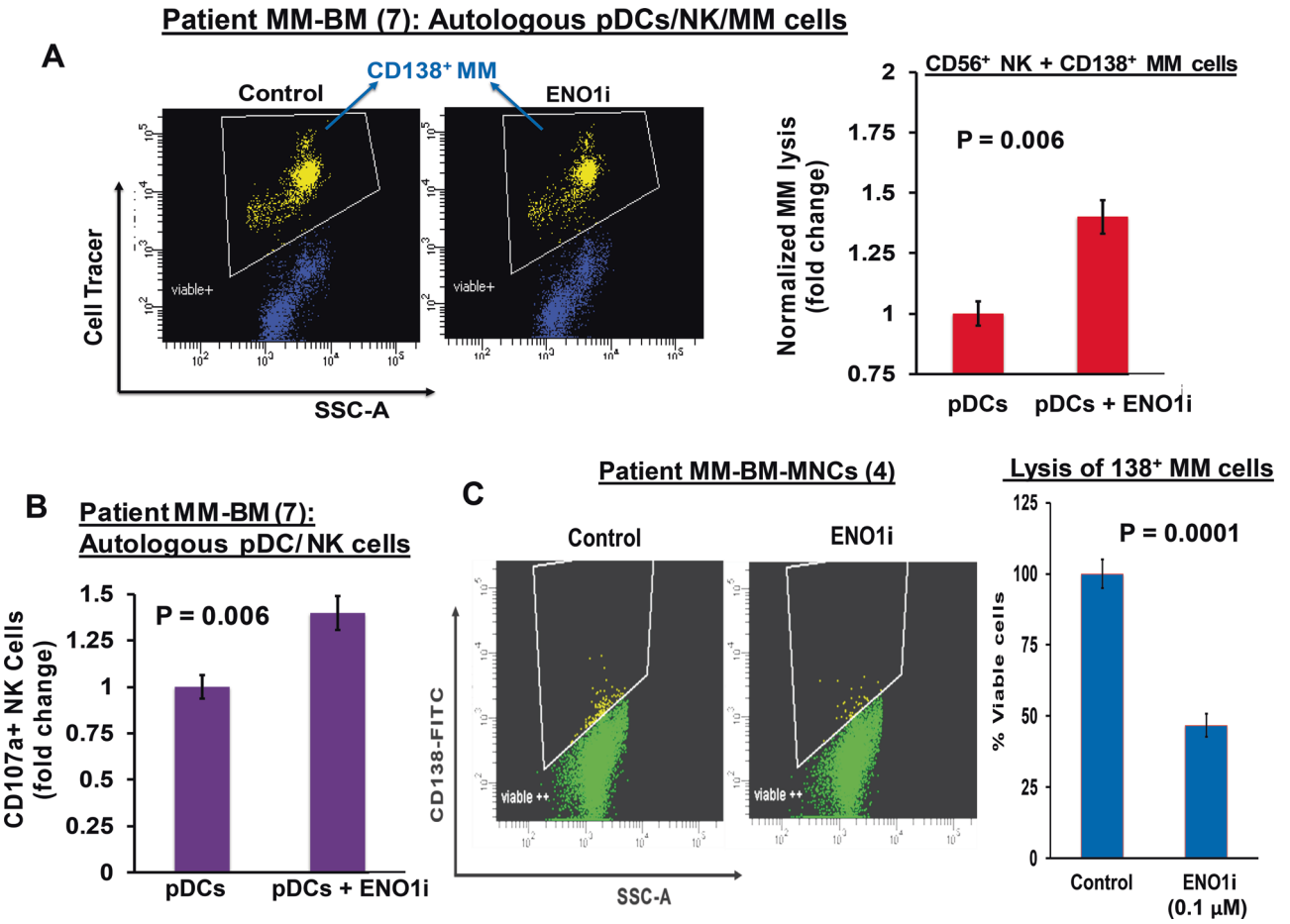

Fig. 5 ENO1 inhibition triggers pDC-induced NK cell-mediated lysis of MM cells. a MM patient BM NK cells were cocultured with autologous pDCs at 1:10 (pDC:NK) ratio in the presence or absence of ENO1i (0.1 μM) for 3 days. After washing to remove ENO1i, cells were cultured for 24 h with autologous MM cells pre-stained with CellTrace violet (10:1 NK:MM ratio), followed by 7-AAD staining and quantification of MM cell lysis by FACS [pDC:NK ratio; 1:10; Effector/Target; 10:1]. Left panel: representative FACS scatter plot showing a decrease in number of viable CellTrace Violet-positive MM cells. Right panel: Bar graph shows quantification of NK-mediated MM cell lysis using data obtained in left panel. The fold change was obtained after normalization with control, and normalized MM cell lysis in the ENO1i-(0.1 μM) treated versus untreated is presented ($N =$ 7 MM patient BM samples; mean ± SD; $p < 0.05$). **b** MM patient pDCs and autologous NK cells (1:10 pDC/NK ratio) were treated with DMSO control or ENO1i (0.1 μM), followed by degranulation assay to assess surface CD107a expression in $CD3^-/CD56^+$ NK cells by multi-parameter flow cytometry. The plot shows percentage of surface $CD107a^+$ NK cells, indicating degranulated cytotoxic NK cells ($N = 7$ MM patient BM samples; mean ± SD; $p < 0.05$). **c** MM patient total BM-MNCs were treated with ENO1i (0.1 μM) for 2 days, and multi-color flow analysis was utilized to assess MM cell lysis. $CD138^+$ MM cells were selected based on their staining of CD138-FITC Ab and quantified. Left panel: representative FACS scatter plot showing a decrease in number of viable FITC-positive MM cells. Right panel: Bar graph shows quantification of $CD138^+$ MM cells in left panel. The fold change was obtained after normalization with control data, and the bar graph is presented as percentage of viable cells in the presence and absence of ENO1i. ($N = 4$ MM patient BM samples; mean ± SD; $p <$ 0.05).

response. As shown in Fig. 6b, the combination of ENO1i plus ACY-241 significantly increased T-cell mediated MM cell lysis compared to either ENO1i or ACY-241 alone (Fig. 6b). Our combination studies of ENO1i with either PD-L1 Ab or ACY-241 therefore suggest potential clinical utility of this combination in MM.

The molecular mechanism(s) whereby pDC-MM interaction-induced ENO1 contributes to immune suppression and tumorigenesis remains to be examined in ongoing studies. Prior studies showed that ENO1-mediated aerobic glycolysis metabolizes glucose into lactate, creating an acidotic tumor-microenvironment and further blunting anti-tumor immune responses [11, 21]. Our data show that pDC-MM interactions induce ENO1, which enhances glycolysis and confers immune dysfunction, as well as promotes MM cell growth and survival, in the BM milieu. This notion is consistent with the "Warburg effect" fostering a tumor microenvironment conducive for MM cell growth. Indeed, preclinical studies have shown efficacy of targeting aerobic glycolysis in cancers including MM [21, 38]. Finally, a recent study showed that lactate dehydrogenase A (LDHA) is associated with drug-resistance in MM [11]; and importantly, that ENO1 gene-

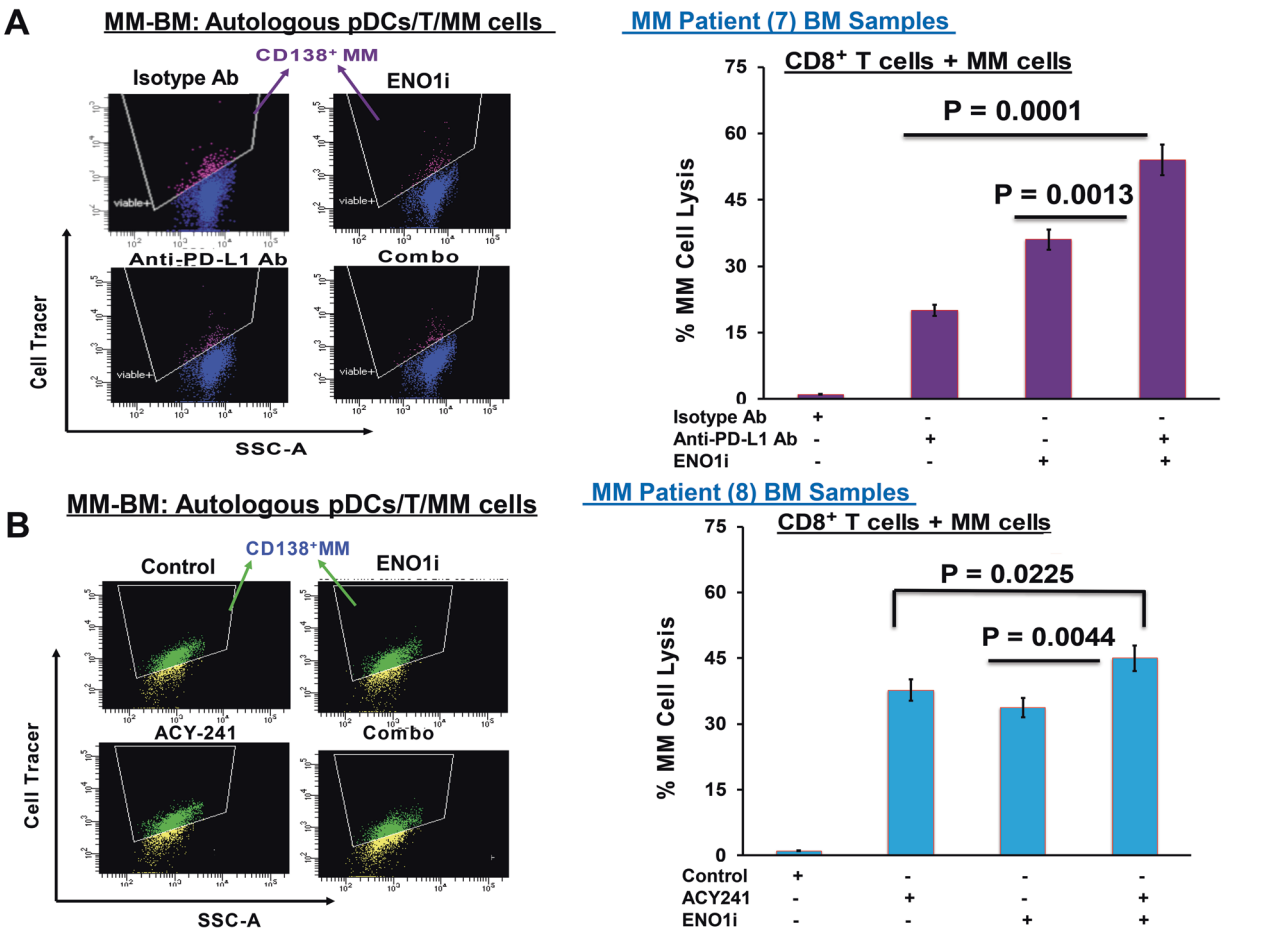

Fig. 6 Combination of ENO1 inhibitor and Anti-PD-L1 Ab or ACY-241 enhances T cell-mediated MM-specific cytotoxic activity. **a** MM patient BM CD8$^+$ T cells ($N = 7$) were co-cultured for 3 days with autologous pDCs (pDC:T; 1:10 ratio) in the presence of anti-PD-L1 Ab (5 μg/ml), ENO1i (0.1 μM), or ENO1i plus anti-PD-L1 Ab. After washing to remove drugs, cells were cultured for 24 h with autologous MM cells pre-stained with CellTrace Violet (T/MM; 10:1 ratio), followed by 7-AAD staining and quantification of CTLs-mediated MM cell lysis by FACS. Left panel: representative FACS scatter plot shows a decrease in number of viable CellTrace Violet-positive MM cells. Right panel: Bar graph shows quantification of CD8$^+$ CTLs-mediated MM cell lysis, reflected in percentage MM cells lysis, using data obtained in left panel. Percentage of MM cell lysis for each treatment versus control (isotype Ab) is presented ($N = 7$ MM patient BM samples; mean ± SD; $p < 0.05$). **b** MM patient BM CD8$^+$ T cells ($N = 8$) were co-cultured for 3 days with autologous pDCs (pDC:T; 1:10 ratio) in the presence of HDAC6 inhibitor ACY-241 (0.1 μM), ENO1i (0.1 μM), or ENO1i plus ACY-241. After washing to remove drugs, cells were cultured for 24 h with autologous MM cells pre-stained with Cell Trace Violet (T/MM; 10:1 ratio), followed by 7-AAD staining and quantification of CTLs-mediated MM cell lysis by FACS. Left panel: representative FACS scatter plot shows a decrease in number of viable CellTrace-positive MM cells. Right panel: Bar graph shows quantification of CD8$^+$ CTLs-mediated MM cell lysis, reflected in percenatge MM cells lysis, using data obtained in left panel. Percentage of MM cell lysis for each treatment versus control is presented ($N = 7$ MM patient BM samples; mean ± SD; $p < 0.05$).

silencing decreases LDHA levels [39]. These findings provide the rationale for targeting ENO1-mediated metabolism to overcome drug-resistance.

In summary, we here show that 1) pDC-MM interactions induce transcription of glycolytic pathway enzyme ENO1 in MM cells; 2) both pDCs and MM cells express ENO1, and pDC-MM interactions further increase ENO1 levels in both cells; 3) ENO1i-activates MM patient pDCs and trigger autologous T cell proliferation; 4) ENO1i induces MM-specific CD8$^+$ CTL activity, as well as NK-cell-mediated cytolytic activity, against autologous MM cells; and, 5) the combination of ENO1i and anti-PD-L1 Ab or HDACi ACY-241 induces more potent MM-specific CD8$^+$ CTL activity against autologous tumor cells than either agent alone. Our preclinical data therefore provide evidence for an immunomodulatory role of ENO1 enzyme in MM, and indicate that therapeutic targeting of ENO1-mediated metabolic pathways using ENO1i, either alone or in combination with anti-PD-L1 Ab (Fig. 7) or ACY-241, will restore host anti-MM immunity, as well as inhibit MM growth and survival in the BM microenvironment.

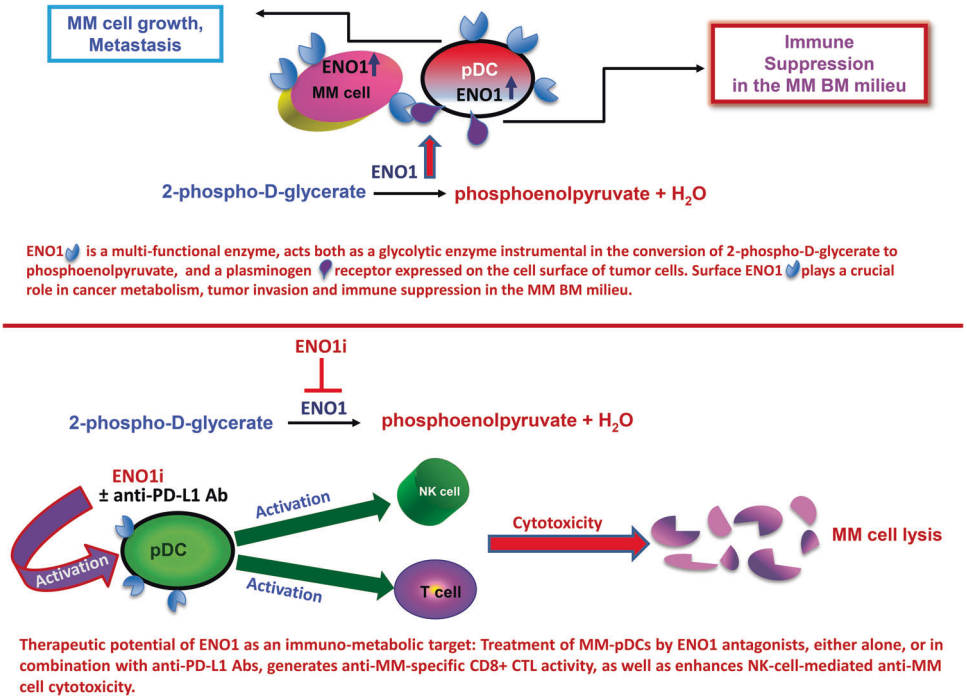

Fig. 7 Schematic representation depicting the role of ENO1 in MM. (Upper panel) pDCs trigger growth, survival, and drug-resistance in MM cells. ENO1 is a multi-functional enzyme, acts both as a glycolytic enzyme instrumental in the conversion of 2-phospho-D-glycerate to phosphoenolpyruvate, and a plasminogen receptor expressed on the cell surface of tumor cells. Surface ENO1 plays a crucial role in cancer metabolism, tumor invasion and immune suppression in the MM BM milieu. ENO1 is upregulated in MM. **(Lower panel) Therapeutic potential of ENO1 as an immuno-metabolic target:** Treatment of MM-pDCs by ENO1 antagonists, either alone, or in combination with anti-PD-L1 Abs, generates anti-MM-specific CD8+ CTL activity, as well as enhances NK-cell-mediated anti-MM cell cytotoxicity.

Materials and methods

Isolation of MM patient BM pDCs, T cells, NK cells, and CD138$^+$ tumor cells

All studies using MM patient samples were performed following IRB-approved protocols at Dana-Farber Cancer Institute/Brigham and Women's Hospital, Boston, USA. Informed consent was obtained from all patients in accordance with Helsinki protocol, and patient samples were de-identified prior to their use in experiments. pDCs were purified from BM using CD304 (BDCA-4/Neuropilin-1) microbeads kit (Miltenyi Biotec). The purity of pDCs (CD3-, CD14-, CD19-, CD20-, CD56-, CD11c-, MHC-II/CD123/BDCA-2$^+$) was confirmed, as previously described [15, 17, 19]. The flow cytometry raw data was analyzed using FACS Diva (BD Biosciences) and FlowJo (Tree Star Inc, USA). MM patient cells were purified (>95% purity) by positive selection using CD138 Microbeads kit. CD8$^+$ T cells and NK cells were purified using negative selection immunomagnetic separation techniques, as previously described [15, 17, 19].

Cell culture and reagents

MM-pDCs were cocultured either in DCP-MM medium (Mattek Corp. Ashland, MA) or complete RPMI-1640 medium supplemented with IL-3 (Peprotech Inc., Rocky Hill, NJ, USA). CD3-PE/FITC/APC; CD4-FITC/PE or APC-Cy7; CD8-APC/FITC, CD56-PE; CD123-PE/PE-Cy5/FITC; and CD138-FITC/PE/APC were obtained from BD Biosciences (San Jose, CA). BDCA-2-FITC and CD11c-APC were obtained from Miltenyi Biotec (Auburn, CA); CD303-, CD304-, CD107a, and PD-L1-BV421 were purchased from Biolegend. Immunomagnetic separation kits were purchased from Miltenyi Biotec. The CellTrace Violet and CellTracker Green flow assay kits were obtained from Life Technologies (USA). PD-L1 blocking antibody (anti-human PD-L1, clone MIH1) was obtained from eBiosciences [19]. HDAC6 inhibitor ACY241 and ENO inhibitor (ENOblock) [40] were purchased from Selleck Chemicals. WST-1 Cell Proliferation Reagent was purchased from Clontech Laboratories, Inc. (USA).

Oligonucleotide arrays

MM cells were co-cultured with pDCs (pDC:MM; 1:5 ratio) for 72 h; MM cells were then separated from the cocultures using CD138 Microbeads, and subjected to Gene Expression analysis using HG-U133 plus 2.0 plus Affymetrix oligonucleotide microarrays [15, 41]. Data processing: the raw data CEL files were obtained using Affymetrix Microarrays Suite 5.0 software. GeneChip 5.0 (Affymetrix, Santa Clara, CA) was utilized to scan, quantify, and analyze the scanned image. GeneChip software automatically calculated intensity values for each probe cell, and marked a presence or absence call for each mRNA. Algorithms in the software used probe cell intensities to calculate an average intensity for each set of probe pairs representing a gene, which correlates with the amount of mRNA. Gene expression patterns for MM cells cultured with or without pDCs were compared, and heat maps were generated (>1.5-fold change in transcripts level was considered significant, CI > 95%). The raw microarray data is provided at the website Gene Expression Omnibus• (http://www.ncbi.nlm.nih.gov/geo/). Accession Number "GSE17407". Gene expression studies were validated at the protein levels using multicolor flow cytometry.

Flow cytometry analysis and cell viability assays

MM cells were cocultured for 24 h with pDCs; cells were then stained with ENO1-FITC and CD138 Abs, followed by multicolor flow analysis to quantify ENO1^{hi} MM cell populations. Cell viability was assessed by WST assay, as previously described [15, 17, 19].

CTL and NK cell activity assays

MM patient BM CD8+ T or NK-cells were cocultured for 3 days with autologous pDCs at 1:10 (pDC:T/NK) ratio, in the presence or absence of ENO1i ENOblock (0.1 μM). After washing to remove the ENO1i, cells were cultured for 24 h with autologous MM cells prestained with CellTrackerViolet (E/T ratio: 10:1, T or NK/MM), followed by 7-AAD staining and quantification of MM cell lysis by FACS. Anti-PD-L1 Ab (5 μg/ml) or ACY-241 (0.2 μM) were utilized for combination studies with ENO1i. CD107a expression was quantified in a degranulation assay. NK-cell mediated cytotoxicity was assessed using flow cytometry-based CFSE-stained MM cell lysis assays, as previously described [17, 19].

Statistical analysis

Statistical significance was obtained using Student's *t*, with the minimal level of significance at p value < 0.05 (Graph Pad PRISM version 6).

Acknowledgements The grant supports for this investigation were provided by "Dr. Miriam and Sheldon Adelson Medical Research Foundation", and by the National Institutes of Health Specialized Programs of Research Excellence (SPORE) grant P50100707, R01CA207237, and RO1 CA050947. KCA is an American Cancer Society Clinical Research Professor.

Author contributions D.C. conceptualized the project, designed research, analyzed data, and wrote the paper; A.R. designed research, performed the experiments, and analyzed the data; Y.S. and T.D. helped in flow cytometry; and K.C.A. provided clinical samples, and reviewed the manuscript.

Compliance with ethical standards

Conflict of interest K.C.A. is on Advisory board of Celgene, Millenium-Takeda, Gilead, Janssen, and Bristol Myers Squibb, and is a Scientific Founder of Oncopep and C4 Therapeutics. D.C. is consultant to Stemline Therapeutic, Inc., and Equity owner in C4 Therapeutics. The remaining authors declare no conflict of interest.

References

1. Anderson KC. The 39th David A. Karnofsky Lecture: bench-to-bedside translation of targeted therapies in multiple myeloma. J Clin Oncol. 2012;30:445–52.
2. Anderson KC. Therapeutic advances in relapsed or refractory multiple myeloma. J Natl Compr Canc Netw. 2013;11:676–9.
3. Anderson KC. Promise of immune therapies in multiple myeloma. J Oncol Pr. 2018;14:411–3.
4. Warburg O, Wind F, Negelein E. The metabolism of tumors in the body. J Gen Physiol. 1927;8:519–30.
5. Gatenby RA, Gillies RJ. Why do cancers have high aerobic glycolysis? Nat Rev Cancer. 2004;4:891–9.
6. Liberti MV, Locasale JW. Metabolism: a new layer of glycolysis. Nat Chem Biol. 2016;12:577–8. https://doi.org/10.1038/nchembio.2133.
7. Vander Heiden MG, Cantley LC, Thompson CB. Understanding the Warburg effect: the metabolic requirements of cell proliferation. Science 2009;324:1029–33. https://doi.org/10.1126/science.1160809.
8. Colegio OR, Chu NQ, Szabo AL, Chu T, Rhebergen AM, Jairam V, et al. Functional polarization of tumour-associated macrophages by tumour-derived lactic acid. Nature 2014;513:559–63. https://doi.org/10.1038/nature13490.
9. Milosevic M, Fyles A, Hedley D, Hill R. The human tumor microenvironment: invasive (needle) measurement of oxygen and interstitial fluid pressure. Semin Radiat Oncol. 2004;14:249–58.
10. Kaelin WG Jr, Ratcliffe PJ. Oxygen sensing by metazoans: the central role of the HIF hydroxylase pathway. Mol Cell 2008;30:393–402. https://doi.org/10.1016/j.molcel.2008.04.009.
11. Maiso P, Huynh D, Moschetta M, Sacco A, Aljawai Y, Mishima Y, et al. Metabolic signature identifies novel targets for drug resistance in multiple myeloma. Cancer Res 2015;75:2071–82. https://doi.org/10.1158/0008-5472.CAN-14-3400.
12. Ikeda S, Kitadate A, Abe F, Takahashi N, Tagawa H. Hypoxia-inducible KDM3A addiction in multiple myeloma. Blood Adv 2018;2:323–34. https://doi.org/10.1182/bloodadvances.2017008847.
13. Ader I, Brizuela L, Bouquerel P, Malavaud B, Cuvillier O. Sphingosine kinase 1: a new modulator of hypoxia inducible

factor 1alpha during hypoxia in human cancer cells. Cancer Res 2008;68:8635–42. https://doi.org/10.1158/0008-5472.CAN-08-0917.
14. Shin YC, Joo CH, Gack MU, Lee HR, Jung JU. Kaposi's sarcoma-associated herpesvirus viral IFN regulatory factor 3 stabilizes hypoxia-inducible factor-1 alpha to induce vascular endothelial growth factor expression. Cancer Res 2008;68:1751–9. https://doi.org/10.1158/0008-5472.CAN-07-2766.
15. Chauhan D, Singh AV, Brahmandam M, Carrasco R, Bandi M, Hideshima T, et al. Functional interaction of plasmacytoid dendritic cells with multiple myeloma cells: a therapeutic target. Cancer Cell 2009;16:309–23.
16. Ray A, Tian Z, Das DS, Coffman RL, Richardson P, Chauhan D, et al. A novel TLR-9 agonist C792 inhibits plasmacytoid dendritic cell-induced myeloma cell growth and enhance cytotoxicity of bortezomib. Leukemia. 2014;28:1716–24.
17. Ray A, Das DS, Song Y, Richardson P, Munshi NC, Chauhan D, et al. Targeting PD1-PDL1 immune checkpoint in plasmacytoid dendritic cell interactions with T cells, natural killer cells and multiple myeloma cells. Leukemia 2015;29:1441–4.
18. Ray A, Das DS, Song Y, Hideshima T, Tai YT, Chauhan D, et al. Combination of a novel HDAC6 inhibitor ACY-241 and anti-PD-L1 antibody enhances anti-tumor immunity and cytotoxicity in multiple myeloma. Leukemia 2018;32:843–6.
19. Ray A, Song Y, Du T, Tai YT, Chauhan D, Anderson KC. Targeting tryptophan catabolic kynurenine pathway enhances anti-tumor immunity and cytotoxicity in multiple myeloma. Leukemia. 2019. https://doi.org/10.1038/s41375-019-0558-x.
20. Bi E, Li R, Bover LC, Li H, Su P, Ma X, et al. E-cadherin expression on multiple myeloma cells activates tumor-promoting properties in plasmacytoid DCs. J Clin Invest 2018;128:4821–31. https://doi.org/10.1172/JCI121421.
21. Cappello P, Principe M, Bulfamante S, Novelli F. Alpha-Enolase (ENO1), a potential target in novel immunotherapies. Front Biosci (Landmark Ed). 2017;22:944–59.
22. Granchi C, Fancelli D, Minutolo F. An update on therapeutic opportunities offered by cancer glycolytic metabolism. Bioorg Med Chem Lett 2014;24:4915–5. https://doi.org/10.1016/j.bmcl.2014.09.041.
23. Ryans K, Omosun Y, McKeithen DN, Simoneaux T, Mills CC, Bowen N, et al. The immunoregulatory role of alpha enolase in dendritic cell function during Chlamydia infection. BMC Immunol 2017;18:27 https://doi.org/10.1186/s12865-017-0212-1.
24. Pacella I, Piconese S. Immunometabolic checkpoints of treg dynamics: adaptation to microenvironmental opportunities and challenges. Front Immunol 2019;10:1889 https://doi.org/10.3389/fimmu.2019.01889.
25. Zhu X, Miao X, Wu Y, Li C, Guo Y, Liu Y, et al. ENO1 promotes tumor proliferation and cell adhesion mediated drug resistance (CAM-DR) in Non-Hodgkin's Lymphomas. Exp Cell Res 2015;335:216–23. https://doi.org/10.1016/j.yexcr.2015.05.020.
26. Barlogie B, Tricot G, Anaissie E, Shaughnessy J, Rasmussen E, van Rhee F, et al. Thalidomide and hematopoietic-cell transplantation for multiple myeloma. N. Engl J Med. 2006;354:1021–30.
27. Muller FL, Colla S, Aquilanti E, Manzo VE, Genovese G, Lee J, et al. Passenger deletions generate therapeutic vulnerabilities in cancer. Nature 2012;488:337–42. https://doi.org/10.1038/nature11331
28. Stessman HA, Baughn LB, Sarver A, Xia T, Deshpande R, Mansoor A, et al. Profiling bortezomib resistance identifies secondary therapies in a mouse myeloma model. Mol Cancer Ther 2013;12:1140–50. https://doi.org/10.1158/1535-7163.MCT-12-1151.
29. Shaughnessy JD Jr, Zhan F, Burington BE, Huang Y, Colla S, Hanamura I, et al. A validated gene expression model of high-risk multiple myeloma is defined by deregulated expression of genes mapping to chromosome 1. Blood 2007;109:2276–84.
30. Vande Broek I, Leleu X, Schots R, Facon T, Vanderkerken K, Van Camp B, et al. Clinical significance of chemokine receptor (CCR1, CCR2 and CXCR4) expression in human myeloma cells: the association with disease activity and survival. Haematologica 2006;91:200–6.
31. Heuck CJ, Qu P, van Rhee F, Waheed S, Usmani SZ, Epstein J, et al. Five gene probes carry most of the discriminatory power of the 70-gene risk model in multiple myeloma. Leukemia 2014;28:2410–3. https://doi.org/10.1038/leu.2014.232.
32. Cappello P, Tonoli E, Roberta Curto R, Giordano D, Giovarelli M, Novelli F. Anti-a-enolase antibody limits the invasion of myeloid-derived suppressor cells and attenuates their restraining effector T cell response. Oncoimmunology. 2016;5:e1112940 https://doi.org/10.1080/2162402X.2015.1112940.
33. Manasanch EE, Han G, Mathur R, Qing Y, Zhang Z, Lee H, et al. A pilot study of pembrolizumab in smoldering myeloma: report of the clinical, immune, and genomic analysis. Blood Adv 2019;3:2400–8. https://doi.org/10.1182/bloodadvances.2019000300
34. Qorraj M, Bruns H, Böttcher M, Weigand L, Saul D, Mackensen A, et al. The PD-1/PD-L1 axis contributes to immune metabolic dysfunctions of monocytes in chronic lymphocytic leukemia. Leukemia 2017;31:470–8. https://doi.org/10.1038/leu.2016.214.
35. Li W, Sun Z. Mechanism of Action for HDAC Inhibitors-Insights from Omics Approaches. Int J Mol Sci. 2019;20:E1616 https://doi.org/10.3390/ijms20071616.
36. Lu C, Zhang K, Zhang Y, Tan M, Li Y, He X, et al. Preparation and characterization of vorinostat-coated beads for profiling of novel target proteins. J Chromatogr A 2014;1372C:34–41. https://doi.org/10.1016/j.chroma.2014.10.098.
37. Bae J, Hideshima T, Tai YT, Song Y, Richardson P, Raje N, et al. Histone deacetylase (HDAC) inhibitor ACY241 enhances anti-tumor activities of antigen-specific central memory cytotoxic T lymphocytes against multiple myeloma and solid tumors. Leukemia 2018;32:1932–47. https://doi.org/10.1038/s41375-018-0062-8.
38. Gu Z, Xia J, Xu H, Frech I, Tricot G, Zhan F. NEK2 promotes aerobic glycolysis in multiple myeloma through regulating splicing of pyruvate kinase. J Hematol Oncol. 2017;10:17 https://doi.org/10.1186/s13045-017-0392-4.
39. Zhao M, Fang W, Wang Y, Guo S, Shu L, Wang L, et al. Enolase-1 is a therapeutic target in endometrial carcinoma. Oncotarget 2015;6:15610–27.
40. Jung DW, Kim WH, Park SH, Lee J, Kim J, Su D, et al. A unique small molecule inhibitor of enolase clarifies its role in fundamental biological processes. ACS Chem Biol 2013;8:1271–82.
41. Chauhan D, Li G, Auclair D, Hideshima T, Richardson P, Podar K, et al. Identification of genes regulated by 2-methoxyestradiol (2ME2) in multiple myeloma cells using oligonucleotide arrays. Blood 2003;101:3606–14.